10572 *Inorg. Chem.* **2009**, *48*, 10572–10580
DOI: 10.1021/ic901063y

Inorganic Chemistry
Article

A Multiconfigurational ab Initio Study of the Zero-Field Splitting in the Di- and Trivalent Hexaquo−Chromium Complexes

Dimitrios G. Liakos, Dmitry Ganyushin, and Frank Neese*

Institute for Physical and Theoretical Chemistry, Bonn University, Wegelerstrasse 12, 53115 Bonn, Germany

Received June 2, 2009

A detailed analysis of the value of zero-field splitting for the di- and trivalent chromium hexaquo complexes is presented. The effect of the Jahn−Teller distortion was studied, for the case of the divalent complex, through the use of state-averaged CASSCF calculations, for the mapping of the potential energy surface along the e_g normal modes. At the minima of the surface, multiconfigurational ab initio calculations (spectroscopy oriented configuration interaction, SORCI, and difference dedicated configuration interaction, DDCI) were used for the calculation of the **D** tensor and the analysis of the individual contributions to it. The final value calculated with the SORCI method ($D = -2.45\ cm^{-1}$) for the divalent complex is in excellent agreement with the experimental estimate ($D = -2.3\ cm^{-1}$). The importance of inclusion of the direct spin−spin coupling contribution to D is pointed out (∼16%). At the same time, contributions of the higher than the lowest $^3T_{1g}$ triplets were found to be non-negligible as well (∼11%). The accuracy of second-order perturbation theory for the calculation of SOC was investigated and found to be satisfactory. For comparison, DFT calculations were performed with hybrid (B3LYP) and nonhybrid (BP86) functionals and were found to be inferior to the wave function based ab initio methods.

Introduction

Magnetic properties of transition metal complexes are, with rare exceptions, well-described by a spin-Hamiltonian (SH) that contains only spin degrees of freedom (for reviews on the history and theory of the SH, see refs 1−3). The associated Schrödinger equations are of low-dimension and can readily be solved exactly or nearly exactly. In order to do so, the introduction of phenomenological parameters (**g** tensor, zero-field splitting, and hyperfine couplings) that must be determined through fitting to experiment is necessary. The geometric and electronic structure content of these values must be clarified by electronic structure theory. Traditionally, this is done by ligand-field theory (LFT) that has shown tremendous success in providing a qualitative guide to the magnetic properties of transition metal ions.[4,5] However, when it comes to truly quantitative interpretations, LFT is not the method of choice. Quite frequently, fitting of the ligand field or essentially ad hoc introduced covalency parameters allows one to obtain agreement with experimental electron paramagnetic resonance (EPR) parameters, but the justification and the reliability of the values assumed in the matching procedure is uncertain.

Today, quantum chemistry has progressed to the point where fairly elaborate electronic structure calculations can be done on reasonably sized molecules, and it is timely to reinvestigate some of the classic systems in order to determine if the ligand field assumptions were correct. One of the assumptions that has invariably been made in the analysis of the zero-field splitting (ZFS) of transition metal complexes is that the contributions from the direct spin−spin coupling (SSC) is negligible, and all ZFS is determined by spin−orbit coupling (SOC). A typical point in case is the high-spin Mn(III) ion where the standard ligand field models based on the SOC between the excited quintet states within the d manifold of the central metal appear to provide a satisfactory explanation for the observed ZFSs. However, in recent years, this assumption has been challenged by ab initio quantum chemistry. Having obtained the ability to directly calculate the SSC on the basis of correlated ab initio wave functions and having developed methods that provide reliable predictions for the spin-flip excitations that are so characteristic of transition metal complexes, it became clear that the quintet−quintet SOC only accounts for about half of the ZFSs of high-spin Mn(III) complexes.[6] However, this is not a general

*To whom correspondence should be addressed. E-mail: neese@thch.uni-bonn.de.

(1) Bleaney, A. A. B. *Electron Paramagnetic Resonance of Transition Ions*; Dover Publications Inc.: New York, 1986; p 911.
(2) Griffith, J. S. *The Theory of Transition-Metal Ions*; Cambridge University Press: London, 1980.
(3) Neese, F.; Munzarova, M. L. Historical Aspects of EPR Parameter Calculations. In *Calculation of NMR and EPR Parameters*; Kaupp, M., Ed.; Wiley: New York, 2004; pp 21−32.
(4) Figgis, B. N.; Hitchman, M. A. *Ligand Field Theory and Its Applications*; Wiley-VCH: New York, 2000.
(5) Ballhausen, C. J. *Introduction to Ligand Field Theory*; McGraw-Hill: New York, 1962.
(6) Neese, F. *J. Am. Chem. Soc.* **2006**, *128*, 10213.

 Published on Web 10/21/2009

conclusion since in other d^N cases the SOC is more dominant than in Mn(III). A point in case is the recently investigated high-spin Co(II) ion in a tetrahedral environment for which neither the spin-flips nor the SSC play an important role,[7] while for distorted octahedral high-spin Mn(II), they do.[8]

We were motivated to the present work by a remark in Griffith's classic book on LFT where he concluded his analysis of the ZFS in $[Cr(H_2O)_6]^{2+}$ with the words "As we obtain a satisfactory interpretation of the observed D with $\rho = 0$ it would be merely an embarrassment to have a large ρ" (ρ is representing the SS contribution to D). We feel that the time is now right to investigate the validity of Griffith's assumptions on the basis of multiconfigurational ab initio quantum chemistry and wish to report our findings for $[Cr(H_2O)_6]^{2+}$. The case of $[Cr(H_2O)_6]^{3+}$, even though less interesting due to the almost perfectly cubic symmetry and the smallness of the associated D value, is also studied. In studying $[Cr(H_2O)_6]^{2+}$, one must deal with the substantial e⊗E Jahn−Teller effect, and consequently considerable attention will be devoted to mapping of the magnetic parameters along the Jahn−Teller distortion axes.

Many structural studies[9−13] have been performed on octahedrally coordinated hexaquo−Cr^{2+} complexes, and all of them agree on an elongated axial Cr−O bond, as expected from the Jahn−Teller theorem.[14] The $Cr-O_{axial}$ bond distance is found experimentally to be close to 2.4 Å and the $Cr-O_{equatorial}$ close to 2.06 Å.[9,13] The value of D at 250 K both from inelastic neutron scattering and from EPR measurements[13] is found to be ~ -2.3 cm^{-1} . The value of E is found to range from ~0.16 to ~0.18 cm^{-1}, depending on the experimental method, for Tutton's salts[13] and less than 0.1 for aqueous Cr^{2+}.[15]

For Cr^{3+}, the corresponding results[16,17] show a structure with six equal bonds of ~1.96 Å complexes and, of course, no Jahn−Teller distortion. Values of D in solutions[18] and crystals[19] have found to be less than 0.1 cm^{-1}.

Computational Details

All calculations were performed with the quantum chemistry program ORCA.[20] Two different structure optimizations were carried out with the B3LYP[21] and BP86[22−24] density functionals in conjunction with the TZVP[25] basis set. The results are collected in Table 1 and show that both methods produce comparable structures. Relativistic effects were treated at the all-electron level with the ZORA method[26] using van Wüllen's model potential idea.[27] The converged structures were verified as minima through numerical frequency calculations using two-sided finite differences.

In order to investigate the Jahn−Teller effect of the divalent chromium ion, calculations were carried out on a grid of $16 \times 32 = 512$ points along the two relevant E_g stretching modes E_ε and E_θ. These were defined as follows: for the oxygen atoms along the $\pm x$, $\pm y$, and $\pm z$ axes, the positions are chosen according to

$$R_z = R_{Oh} + 2R_\theta$$
$$R_x = R_{Oh} - R_\theta + R_\varepsilon$$
$$R_y = R_{Oh} - R_\theta - R_\varepsilon$$

Here, R_θ and R_ε are the displacement parameters (in Ångström units) used to reproduce the changes in the Cr−O bonds distances across the E_g normal modes of vibration, and R_{Oh} is the mean Cr−O distance for a hypothetical perfectly cubic structure (taking account of the protons, the highest possible symmetry for a hexaquo complex is T_h). Negative values of R_ε simply lead to an interchange of the x and y axes such that the values corresponding to negative R_ε are readily obtained from those already calculated for positive R_ε.

At each point on the grid, a state averaged CASSCF (CAS(n,5) $n = 3$ for Cr(III) and $n = 4$ for Cr(II)) calculation was performed where the five active orbitals are the metal d-based ones. For the Cr(III) complex, the calculations were averaged over all 10 quartet and 35 doublet roots and for the Cr(II) case over all five quintet and 35 triplet states. Additionally for the case of Cr(II), we performed a second set of calculations on a larger grid of $16 \times 42 = 672$ points, again using the state averaged CASSCF method, with the five quintet and the eight most important triplets states. In this latter set of calculations we also increased the size of the basis set through to TZVPP. Unless otherwise noted, the CASSCF results will refer to this choice. At the stationary points (minima or maxima) found on the CASSCF surfaces, more accurate multireference correlation calculations were performed. Specifically, the multireference difference dedicated configuration interaction (MR-DDCI2[28]) and spectroscopy-oriented CI (SORCI[29]) methods were employed. For the individually selecting MR methods, the selection threshold T_{sel} was 10^{-6} Eh, the prediagonalization threshold T_{pre} was set to 10^{-4}, and the natural orbital truncation threshold T_{nat} was 10^{-5} Eh.[29] In the case of MR methods, both the TZVP and the more extensively polarized TZVPP basis sets were used.

For the calculation of the ZFS properties, the spin−orbit mean field (SOMF)[30−32] approximation was used to approximate the Breit−Pauli two-electron SOC operator. As will be explained below, both second-order perturbation theory[33] as

(7) Sundararajan, M.; Ganyushin, D.; Shengfa, Y.; Neese, F. *J. Chem. Soc., Dalton Trans.* **2009**, *30*, 5805−6064.
(8) Duboc, C.; Collomb, M.-N.; Pecaut, J.; Deronzier, A.; Neese, F. *Chem.—Eur. J.* **2008**, *14*, 6498.
(9) Figgis, B. N.; Kucharski, E. S.; Reynolds, P. A. *Acta Crystallogr.* **1990**, *B46*, 577.
(10) Figgis, B. N.; Kucharski, E. S. *Acta Crystallogr.* **1991**, *C47*, 419.
(11) Araya, M. A.; Cotton, F. A.; Daniels, L. M.; Falvello, L. R.; Murillo, C. A. *Inorg. Chem.* **1993**, *32*, 4853.
(12) Cotton, F. A.; Daniels, L. M.; Murillo, C. A.; Quesada, J. F. *Inorg. Chem.* **1993**, *32*, 4861.
(13) Dobe, C.; Noble, C.; Carver, G.; Tregenna-Piggot, P. L. W.; McIntyre, G. J.; Barra, A.-L.; Neels, A.; Juranyi, F. *J. Am. Chem. Soc.* **2004**, *126*, 16639.
(14) Jahn, H. A.; Teller, E. *Proc. R. Soc. London* **1937**, *161*, 220.
(15) Telser, J.; Pardi, L. A.; Krzystek, J.; Brunel, L.-C. *Inorg. Chem.* **1998**, *37*, 5769.
(16) Beattie, J. K.; Best, S. P.; Skelton, B. W.; White, A. H. *J. Chem. Soc., Dalton Trans.* **1981**, 2105.
(17) Best, S. P.; Forsyth, J. B. *J. Chem. Soc., Dalton Trans.* **1991**, 1721.
(18) Vishnevskaya, G. P.; Kozyrev, B. M. *J. Struct. Chem.* **1966**, *6*, 637.
(19) Manoogian, A.; Leclerc, A. *J. Chem. Phys.* **1976**, *64*, 4504.
(20) Neese, F. *ORCA*; University of Bonn: Bonn, Germany, 2007.
(21) Becke, A. D. *J. Chem. Phys.* **1993**, *98*, 1372.
(22) Perdew, J. P. *Phys. Rev. B* **1986**, *33*, 8822.
(23) Perdew, J. P. *Phys. Rev. B* **1986**, *34*, 7406.
(24) Becke, A. D. *Phys. Rev. A* **1988**, *38*, 3098.
(25) Schäfer, A.; Huber, C.; Ahlrichs, R. *J. Chem. Phys.* **1994**, *100*, 5829.
(26) Van Lenthe, E.; Snijders, J. G.; Baerends, E. J. *J. Chem. Phys.* **1996**, *105*, 6505.
(27) van Wüllen, C. *J. Chem. Phys.* **1998**, *109*, 392.
(28) Miralles, J.; Castell, O.; Caballol, R.; Malrieu, J.-P. *Chem. Phys.* **1993**, *172*, 33.
(29) Neese, F. *J. Chem. Phys.* **2003**, *119*, 9428.
(30) Hess, B. A.; Marian, C. M.; Wahlgren, U.; Gropen, O. *Chem. Phys. Lett.* **1996**, *251*, 365.
(31) Berning, A.; Schweizer, M.; Werner, H. J.; Knowles, P. J.; Palmieri, P. *Mol. Phys.* **2000**, *98*, 1823.
(32) Neese, F. *J. Chem. Phys.* **2005**, *122*, 34107.
(33) Neese, F.; Solomon, E. I. *Inorg. Chem.* **1998**, *37*, 6568.

Table 1. Cr−O Bond Lengths (Å) Calculated with B3LYP and BP86 Functionals and the TZVP Basis Set

	$Cr(H_2O)_6^{2+}$		$Cr(H_2O)_6^{3+}$	
method	Cr−O_{axial} (Å)	Cr−$O_{equatorial}$ (Å)	Cr−O_{axial} (Å)	Cr−$O_{equatorial}$ (Å)
BP86	2.402	2.088−2.096	2.019	2.019
B3LYP	2.390	2.109−2.114	2.0195	2.019
Exp	∼2.39[13]	∼2.065[13]	1.960[·]	1.960[·]

well as quasi-degenerate perturbation theory (QDPT)[34] were used to this end. The SOMF operator can be written as[32] $\hat{H}_{SOMF} = \sum_i z(i)\,\hat{s}(i)$, and in the second quantization formalism, it becomes

$$\hat{H}_{SOMF} = \frac{1}{2}\sum_{pq} z_{pq}^{-} a_p^{+} b_q + z_{pq}^{+} b_p^{+} a_q + z_{pq}^{0}[a_p^{+} a_q - b_p^{+} b_q] \tag{1}$$

where a_p^{+} is the creation operator for orbital p with $m_s = 1/2$, b_q is the annihilation operator for orbital q with $m_s = -1/2$, and accordingly for the rest operators of this form $z_{pq}^{\pm} = z_{pq}^{x} \pm i z_{pq}^{y}$ and the matrix elements of z are[35]

$$\langle\varphi_\mu|\hat{z}|\varphi_\nu\rangle = \langle\varphi_\mu|\hat{h}^{SOC}|\varphi_\nu\rangle + (\varphi_\mu\varphi_\nu|\hat{g}^{SOC}|\rho) - \frac{3}{2}\sum_{\kappa\tau} P_{\kappa\tau}[(\varphi_\mu\varphi_\kappa|\hat{g}^{SOC}|\varphi_\tau\varphi_\nu) + (\varphi_\tau\varphi_\nu|\hat{g}^{SOC}|\varphi_\mu\varphi_\kappa)] \tag{2}$$

where $\rho(r) = \sum_{\mu,\nu} P_{\mu\nu}\,\phi_\mu(r)\,\phi_\nu(r)$ is the electron density and $P_{\kappa\tau}$ the total charge density matrix. One last step in the construction of the Hamiltonian matrix that has to be diagonalized is the use of the Wigner−Eckart theorem that drastically reduces the number of matrix elements that need to be calculated.[36]

The components of the **D** tensor through the use of second-order perturbation theory have been shown to be[33]

$$D_{kl}^{SOC-(0)} = -\frac{1}{S^2}\sum_{b(S_b=S)} \Delta_b^{-1}\langle 0SS|\sum_i z_{k;i}^{SOMF}\hat{s}_{i;z}|bSS\rangle\langle bSS|\sum_i z_{l;i}^{SOMF}\hat{s}_{i;z}|0SS\rangle \tag{3}$$

$$D_{kl}^{SOC-(-1)} = -\frac{1}{S(2S-1)}\sum_{b(S_b=S-1)} \Delta_b^{-1}\langle 0SS|\sum_i z_{k;i}^{SOMF}\hat{s}_{i;+1}|b(S-1)(S-1)\rangle\langle b(S-1)(S-1)|\sum_i z_{l;i}^{SOMF}\hat{s}_{i;-1}|0SS\rangle \tag{4}$$

$$D_{kl}^{SOC-(+1)} = -\frac{1}{(S+1)(2S+1)}\sum_{b(S_b=S+1)} \Delta_b^{-1}\langle 0SS|\sum_i z_{k;i}^{SOMF}\hat{s}_{i;-1}|b(S+1)(S+1)\rangle\langle b(S+1)(S+1)|\sum_i z_{l;i}^{SOMF}\hat{s}_{i;+1}|0SS\rangle \tag{5}$$

where the first term describes contributions from excited states of the same spin as the ground state ($S' = S$), the second term arises from states with $S' = S-1$, and finally the third term arises from states with spin $S' = S+1$. Here, k and l denote Cartesian components x, y, and z, and Δ_b is the energy difference between the ground state and the bth excited state in the absence of the SOC interaction.

The SSC contribution to the ZFS was evaluated directly over the multireference wave function with no further approximation to the integrals or coupling coefficients.[34,35] The final formulas for the calculation of the matrix elements of the SSC coupling operator are:

$$\langle aSM|\hat{H}_{ssc}|a'SM'\rangle = \frac{\sqrt{(S+1)(2S+3)}}{\sqrt{S(2S-1)}}\begin{pmatrix} S' & 2 & S \\ M' & 0 & M \end{pmatrix}\sum_{pqrs} D_{pqrs}^{(m)}\langle aSS|Q_{pqrs}^{0}|a'SS\rangle \tag{6}$$

with $Q_{pqrs}^{(0)} = {}^1/_4\sqrt{6}\{E_{pq}\delta_{sr} - S_{pq}^{z}S_{rs}^{z} - E_{pq}E_{rs}\}$ representing a special two electron spin density, and $D_{pqrs}^{(0)} = \frac{1}{\sqrt{6}}\int\int \varphi_p(r_1)\,\varphi_r(r_2)\,\frac{3r_{12z}r_{2z}-r_1r_2}{r_{12}^5}\,\varphi_q(r_1)\,\varphi_s(r_2)\,dr_1\,dr_2$ denotes the two-electron field gradient integrals and the excitation operator $\hat{E}_{pq}$ and $\hat{S}_{pq}$ defined through $\hat{E}_{pq} = \hat{a}_p^{\dagger}\hat{a}_q + \hat{b}_p^{\dagger}\hat{b}_q$ and $\hat{S}_{pq}^{z} = \hat{a}_p^{\dagger}\hat{a}_q - \hat{b}_p^{\dagger}\hat{b}_q$. As for the SOC, the SSC term can be included either by finite-order (in this case first-order) or quasi-degenerate perturbation theory, as will be discussed below.

Results and Analysis

Jahn−Teller Effect. $Cr(H_2O)_6^{2+}$ as a high-spin d^4 complex has a ^5D ground spectroscopic term. Under O_h symmetry, this term is split to $^5T_{2g}$ and ^5E_g, with ^5E_g being lower in energy. The Jahn−Teller theorem[14] assures that the complex will distort spontaneously into a lower energy orbital nondegenerate configuration, typically by an axial elongation. This is consistent with the calculated geometry that yielded two sets of Cr−O distances (axial ∼2.39 Å, equatorial∼2.09 Å) in agreement with the experimental findings (Table 1). The Cr(II) high-spin d^4 configuration is subject to the well-known E⊗e Jahn−Teller coupling case; for example, the E_g electronic state couples to e_g molecular vibrations in order to break the electronic degeneracy.

We will follow the accepted practice to term the two members of the vibrational e_g set Q_θ and Q_ε. They transform as $Q_\theta \sim 3z^2 - r^2$ and $Q_\varepsilon \sim x^2 - y^2$ and can be expressed through Cartesian coordinates in the form[37] $Q_\theta \sim (2Z_1 - 2Z_4 - X_2 + X_5 - Y_3 + Y_6)/(2\sqrt{3})$ and $Q_\varepsilon \sim (1/2)(X_2 - X_6 + Y_3 + Y_6)$ (Figure 1). In this form, omitting the normalization constants, we describe the two vibrations using internal coordinates.

(34) Ganyushin, D.; Neese, F. *J. Chem. Phys.* **2008**, *128*, 114117.
(35) Ganyushin, D.; Neese, F. *J. Chem. Phys.* **2006**, *125*, 024103.
(36) Neese, F.; Solomon, E. I. *Magnetoscience - From Molecules to Materials*; Miller, J. S., Drillon, M., Eds.; Wiley VCH: Weinheim, Germany, 2003; Vol. *IV*.
(37) Bersuker, I. B. *The Jahn-Teller Effect*; Cambridge University Press: Cambridge, U. K., 2006.

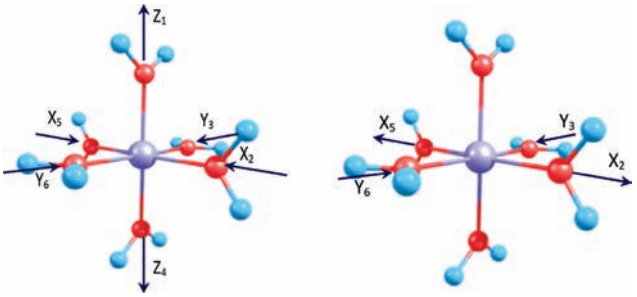

Figure 1. Schematic description of the two vibrations of E_g symmetry. The left one refers to Q_θ and the right to Q_ε.

For the E⊗e problem at hand, the linear terms in the vibronic coupling operator lead to two energy levels with energies[37]

$$\varepsilon_\pm(\rho) = \frac{1}{2}K_E\rho^2 \pm |F_E|\rho$$

Here, the two vibrations have been parametrized by $Q_\theta = \rho\cos\varphi$ and $Q_\varepsilon = \rho\sin\varphi$, K_E is the force constant for the e_g mode, and F_E is the linear vibronic coupling constant. The minimum energy occurs at a distance $\rho_{JT} = |F_E|/K_E$. Thus, the energy minima of the two vibronic energy levels do not depend on the angle φ, and the potential has the well-known "Mexican hat" shape. After inclusion of quadratic terms, the potential energy surfaces become[37]

$$\varepsilon_\pm(\rho,\varphi) = \frac{1}{2}K_E\rho^2 \pm \rho[F_E^2 + G_E^2\rho^2 + 2F_EG_E\rho\cos(3\varphi)]^{1/2} \quad (7)$$

An explicit dependence on the angle φ is now apparent. Minimization of these energy levels leads to

$$\rho_0 = \frac{\pm F_E}{K_E\mu(-1)^n 2G_E}, \varphi_0 = \frac{n\pi}{3}, n = 0, 1, ..., 5 \quad (8)$$

$$E_{JT} = \frac{F_E^2}{2(K_E - 2|G_E|)} \quad (9)$$

$$\delta = \frac{4E_{JT}|G_E|}{K_E + 2|G_E|} \quad (10)$$

G_E is the quadratic vibronic constant, and δ is the minimum barrier between the three minima. The calculated E_{JT} at the CASSCF/TZVP level (simply the energy difference between the undistorted and distorted minimum energy structures) was found to be 954 cm^{-1}. This result is close to the one previously calculated by Aakesson et al.[38] (888 cm^{-1}) but is an underestimate compared to the experimental analysis[13] that predicts a value around 1600 cm^{-1}. This value was improved upon introduction of the extensively polarized TZVPP basis set, to 1082 cm^{-1}. As anticipated, the multireference calculations provided slightly larger values that are collected in Table 2. From Figure 2, one observes that the three minima that correspond to $n = 0, 2$, and 4 are located at a value of $\rho = 0.24$ Å. This value of the Jahn−Teller radius agrees with the one calculated earlier through ab initio coupled pair functional calculations.[38] It is also evident that the minimum energy path that connects the three minima is at −907 cm^{-1}, such that the energy barrier is found to be 1082 − 907 = 175 cm^{-1} at the CASSCF level of theory. By solving eqs 8−10, one determines the linear vibronic constant F_E = −0.179 mdyne, the quadratic vibronic constant G_E = −0.036 mdyne $Å^{-1}$, and K_E = 0.818 mdyne $Å^{-1}$. With this value of K_E, we obtain a value of 278 cm^{-1} for $\hbar\omega$. The corresponding value used in two recent experimental works is 254 cm^{-1}.[13,39] Nevertheless, for this nice agreement, between the two K_E values, a cancellation of two deviations between the calculated and experimentally derived numbers is also responsible. The value of E_{JT} used by Dobe et al. is close to 1600 cm^{-1} in order to reproduce the observed optical transition around 8000 cm^{-1} that is assigned to the transition between the tetragonally split components of the ^5E_g (O_h) ground term,[13] keeping in mind that some ∼1500 cm^{-1} are due to strain effects. From the data in Table 2, it appears that the SA-CASSCF calculations underestimate the value of this splitting, giving an energy difference of 4625 cm^{-1}. This value is improved at the SORCI level, where nevertheless it is still too small. This is due to the smaller Jahn−Teller radius predicted by the calculations compared to the one estimated experimentally. However, when a SORCI calculation was performed at the experimentally determined radius, the energy splitting rose to 6600 cm^{-1}, which is in excellent agreement with the experimentally observed transition energy. Thus, the calculations are in good agreement with the experimentally deduced force constants. It should be noted here that the ^5E_g state, due to symmetry reasons, gives no contribution to the value of D, and so this small underestimation of its energy splitting should have no influence on the calculation of ZFS.

In $Cr(H_2O)_6^{3+}$, the electronic configuration of Cr is d^3 and gives rise to a ^4F ground term that, under the influence of the O_h ligand field, splits into the orbitally nondegenerate $^4A_{2g}$ ground as well as two triply degenerate $^4T_{1g}$ and $^4T_{2g}$ excited terms. The geometry optimizations yielded Cr−O distances of 2.0 Å, in fair agreement with experimental results.[16,17]

Table 2. Jahn−Teller Energy for $Cr(H_2O)_6^{2+}$ and the Energy Splitting of the ^5E_g Ground Term in the Energy Minimum of the CASSCF/TZVPP Surface with Different Methods of Calculation[a]

Method	E_{JT} (cm^{-1})	splitting of the ^5E_g term (cm^{-1})
CASSCF(TZVP)	954	3984
CASSCF(TZVPP)	1082	4625
MRDDCI2(TZVP)	1188	4318
MRDDCI2(TZVPP)	1457	4483
SORCI(TZVP)	1340	4485
SORCI(TZVPP)	1708	4630
exptl[13]	∼1600	∼6500

[a] For CASSCF, the 4d electrons were used and the 5d orbitals together with the TZVP and TZVPP basis set. For the SORCI and the MR-DDCI2, we used the TZVP and also TZVPP basis sets. For the CASSCF/TZVP case, the calculations refer to the minimum of its own surface.

Comparison between Theory and Experiment at the Minimum Energy Geometries. The DFT geometry optimization with both B3LYP and BP86 functionals gave two-sets of bond distances for $Cr(H_2O)_6^{2+}$. As can be seen

(38) Aakesson, R.; Pettersson, L. G. M.; Sandstroem, M.; Wahlgren, U. *J. Phys. Chem.* **1992**, *96*, 150.

(39) Carver, G.; Thut, M.; Noble, C.; Tregenna-Piggott, P. L. W. *J. Chem. Theory Comput.* **2008**, *4*, 603.

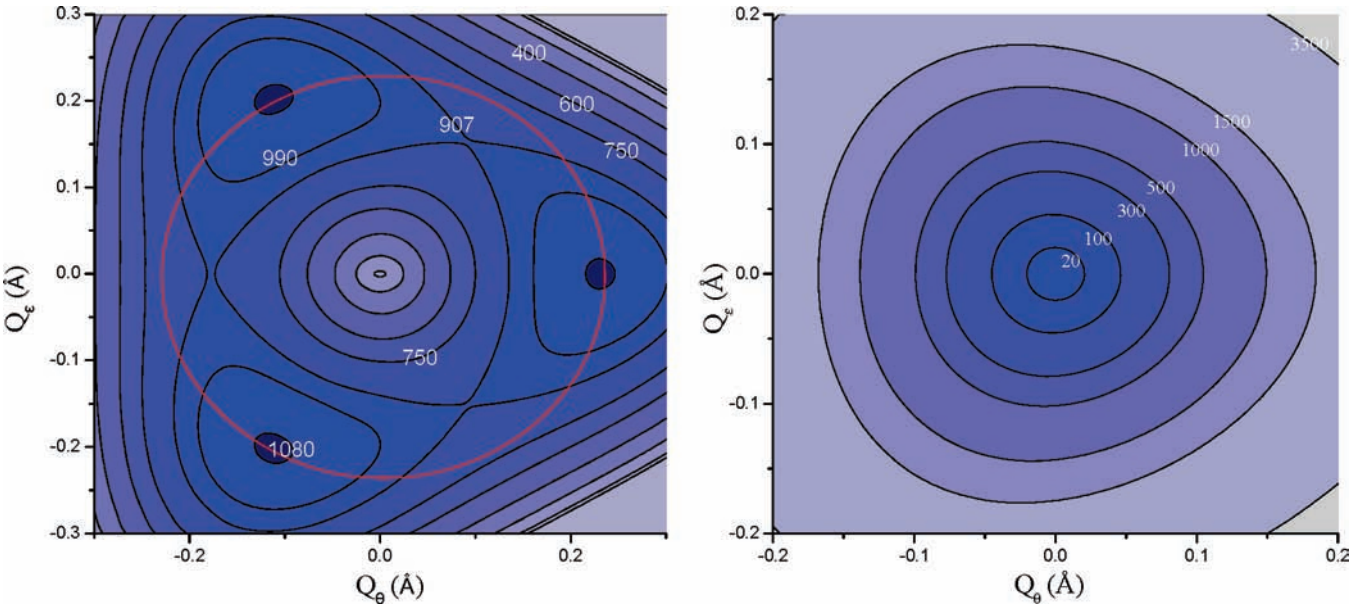

Figure 2. Potential energy surface for the two vibrations of E_g symmetry. The left one refers to $Cr(H_2O)_6^{2+}$ and the right one to $Cr(H_2O)_6^{3+}$. The calculations were performed using CASSCF(4,5) for the complex with a charge of +2 and CASSCF(3,5) for the complex with a charge of +3. (TZVP basis set for charge +3 and TZVPP for charge +2.)

from Table 1, the difference between theory and experiment for the axial Cr−O bonds is ~0.01 Å, while for the equatorials it is at most ~0.049 Å.

The value of D calculated at this point is $-2.45\ cm^{-1}$ at the SORCI/TZVPP level of theory, which is in excellent agreement with the experimental value of $D = -2.2\ cm^{-1}$.[15] At the experimentally determined JT radius, a D value of $-2.34\ cm^{-1}$ was calculated with SORCI/TZVPP, which should be taken as our best theoretical result. The calculated value of E was $0.04\ cm^{-1}$, also in agreement with the experimental estimate of less than $0.1\ cm^{-1}$.[15] The existence of a finite value for E cannot be explained in the framework of σ bonding, where a value of 0 should be obtained. Nevertheless, as has been showed by Tregenna-Piggott et al.,[40] this result can be explained, in the case of the isoelectronic $Mn[H_2O]_6^{3+}$, as a consequence of anisotropic π interactions between the central metal and the water ligands.

For the trivalent complex, a value of zero at the fully symmetric geometry was calculated, while[19] some values of less than $0.1\ cm^{-1}$ have been reported for some chromic alums due to small trigonal distortions.

Quasi-Degenerate versus Second-Order Perturbation Theory. As the ground state of the divalent hexaquo chromium complex is orbitally degenerate, SOC effects are potentially large, and perturbation theory may not be appropriate for the determination of the **D** tensor. This subject is investigated in this section, where QDPT is compared to the closed-form perturbation expressions for the **D** tensor.[33]

The matching is best done by first solving the SH in closed form and then comparing the eigenvalues with those calculated by the QDPT procedure. This comparison has the potential flaw that the QDPT procedure includes higher than biquadratic terms in the effective spin, but those terms are omitted from the SH. Nevertheless, the error introduced by this approximation must remain minor, as the higher-order terms are known to be much smaller than their biquadratic counterparts.[41]

For $S = 2$, the matrix representation of the ZFS term in the SH is

$$H_{ZFS} = \begin{pmatrix} 2D & \sqrt{6}E & 0 & 0 & 0 \\ \sqrt{6}E & -2D & \sqrt{6}E & 0 & 0 \\ 0 & \sqrt{6}E & 2D & 0 & 0 \\ 0 & 0 & 0 & -D & 3E \\ 0 & 0 & 0 & 3E & -D \end{pmatrix} \quad (11)$$

The eigenvalues and eigenfunctions are known to be[42]

$$E_{1s} = -D + 3E \quad |1^s\rangle = \frac{\sqrt{2}}{2}(|1,1\rangle + |1,-1\rangle) \quad (12)$$

$$E_{1a} = -D - 3E \quad |1^a\rangle = \frac{\sqrt{2}}{2}(|1,1\rangle - |1,-1\rangle) \quad (13)$$

$$E_{2a} = 2D \quad |2^a\rangle = \frac{\sqrt{2}}{2}(|2,2\rangle - |2,-2\rangle) \quad (14)$$

$$E_{2s} = 2\sqrt{D^2 + 3E^2}$$
$$|2^s\rangle = a^+\frac{\sqrt{2}}{2}(|2,2\rangle + |2,-2\rangle) + a^-|2,0\rangle \quad (15)$$

$$E_0 = -2\sqrt{D^2 + 3E^2}$$
$$|0'\rangle = a^-\frac{\sqrt{2}}{2}(|2,2\rangle + |2,-2\rangle) - a^+|2,0\rangle \quad (16)$$

(40) Tregenna-Piggott, P. L. W.; Weihe, H.; Barra, A.-L. *Inorg. Chem.* **2003**, *42*, 8504.

(41) Krzystek, J.; Ozarowski, A.; Telser, J. *Coord. Chem. Rev.* **2006**, *250*, 2308.

(42) Hendrich, M. P.; Debrunner, P. G. *Biophys. J.* **1989**, *56*, 489.

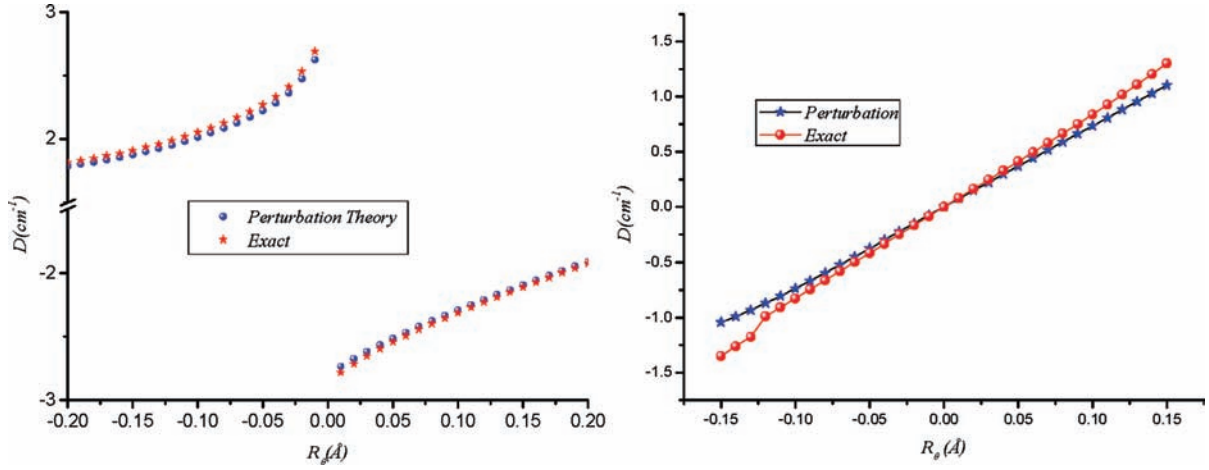

Figure 3. Comparison of the exact D values and the ones calculated through perturbation theory for the two complexes. The left one refers to $Cr(H_2O)_6^{2+}$ and the right one to $Cr(H_2O)_6^{3+}$.

with

$$a^{\pm} = \frac{1}{4}\sqrt{1 \pm D/\sqrt{D^2 + 3E^2}} \qquad (17)$$

For $S = 3/2$, the SH matrix is

$$H_{ZFS} = \begin{pmatrix} D & \sqrt{3}E & 0 & 0 \\ \sqrt{3}E & -D & 0 & 0 \\ 0 & 0 & -D & \sqrt{3}E \\ 0 & 0 & \sqrt{3}E & D \end{pmatrix} \qquad (18)$$

The eigenvalues and eigenfunctions are readily determined.[43]

The energy differences between the analytic eigenvalues can be matched with the ones obtained from the QDPT procedure in order to obtain values for D and E. These can then be compared with the ones obtained from second-order perturbation theory (eqs 3−5). The comparison between the two sets of theoretical D values is shown in Figure 3 for the di- and trivalent hexaquo−chromium complexes for a cut along the Q_θ vibrational mode ($Q_\varepsilon = 0$).

It is obvious that in both cases second-order perturbation theory is fully adequate for the calculation of the **D** tensor. In the case of $Cr(H_2O)_6^{2+}$, the deviation is 1.4% or 0.033 cm^{-1} across the θ normal mode of vibration. For the case of $Cr(H_2O)_6^{3+}$, the corresponding values are 10.4% and 0.08 cm^{-1}. This is expected for the trivalent complex but also holds along the entire potential energy surface in the divalent case since the E state has no in-state SOC. The calculations provide some idea about the magnitude of the distortion that is necessary in the trivalent case in order to arrive at the experimentally observed D value of 0.1 cm^{-1}. Already, distortions of about 0.02 Å are enough to induce such a ZFS. Hence, one can infer that the trivalent hexaquo−chromium complex adopts an average configuration in solution that is quite close to cubic.

Individual Contributions to the D Value. Spin−Spin Contribution. The decomposition of the D value into SOC and SSC contributions as a function of the Q_θ coordinate is shown in Figure 4.

In both cases, the SSC is essentially geometry-independent and considerably smaller than the SOC contribution (essentially zero for the Cr(III) complex and 0.371 cm^{-1} for the Cr(II) complex). The change in sign going from elongation to compression is due to a z-axis change so that the condition $0 \le E/D \le 1/3$ is still valid. Since the hexaquo complexes generally have a very limited covalency, this is a sensible result. As long as there is no significant geometry-dependent d/p mixing or covalent delocalization, there is no a priori reason for the SSC contribution to vary in a pronounced way with geometry changes. The fact that the SSC is geometry independent also demonstrates that the first-order SSC effects are dominant and provides an a posteriori justification for the use of first-order perturbation theory for this term. Taken together, these results show that Griffith was essentially right to dismiss the SSC contribution as a major contributor to the ZFS in hexaquo-chromium complexes. The contribution of the SSC in the Cr(II) case is ~15% of the total value of D. This means that it must be included for true quantitative accuracy but can be ignored for a qualitative discussion. Our results remain unchanged upon repeating the calculations with the MR-DDCI2 or SORCI methods in place of SA-CASSCF. Detailed numbers are documented in Table 3.

Analysis of Excited State Contributions to the SOC Term. The effective geometry of the divalent chromium−hexaquo complex in all of its three minima is D_{2h}. In this point group, the three components of angular momentum transform as[44] L_x, B_{3g}; L_y, B_{2g}; and L_z, B_{1g}. It is readily determined that both T_{1g} and T_{2g} states in O_h symmetry map onto $B_{1g} + B_{2g} + B_{3g}$ states under D_{2h} and hence can both spin−orbit-couple with the ground state. An actual calculation is shown in Figure 5, where a scan along the Q_θ coordinate is reported. A qualitative energy splitting diagram is shown in Figure 6 for the two main cases of axial elongation and axial compression. The energies of the excited states at the SORCI/TZVPP level

(43) Mabbs, F. E.; Collison, D. *Electron Paramagnetic Resonance of d Transition Metal Compounds*; Elsevier: New York, 1993.

(44) Herzberg, G. *Molecular Spectra and Molecular Structure Volume III - Electronic Spectra and Electronic Structure of Polyatomic Molecules*, 2nd ed.; Krieger Publishing Company: Malabar, FL, 1966.

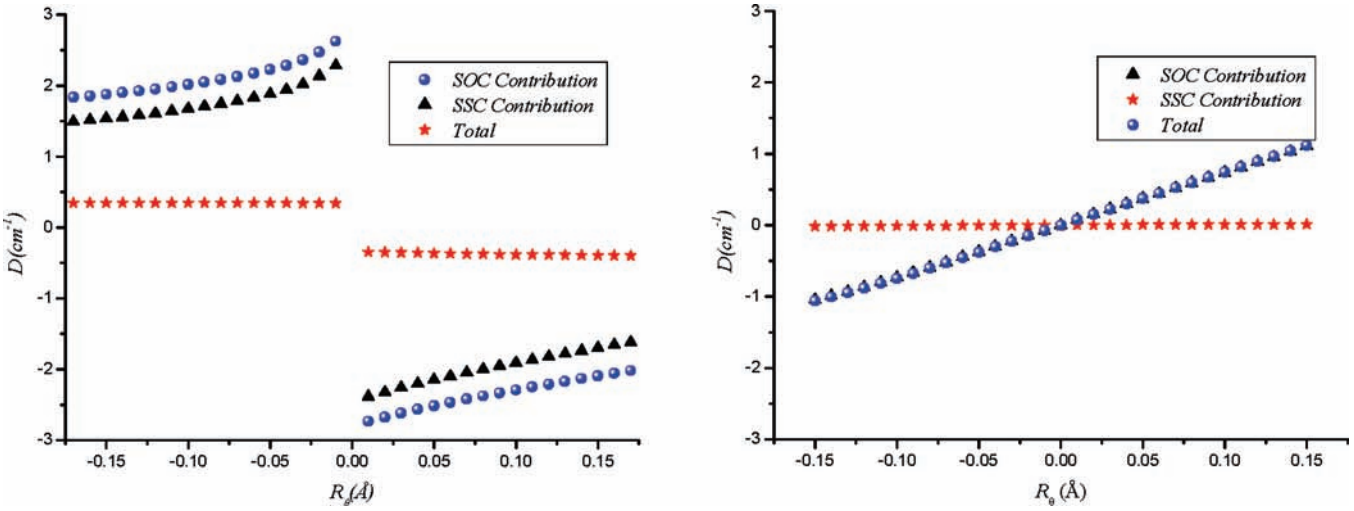

Figure 4. Contribution of direct spin−spin coupling to the total value of D as a function of the Q_θ coordinate. Left: $Cr(H_2O)_6^{2+}$. Right: $Cr(H_2O)_6^{3+}$.

Table 3. Decomposition of the Total Value of D with Various Methods of Calculation

	CASSCF (TZVPP)	SORCI (TZVPP)	MR-DDCI2 (TZVPP)
SOC-triplets	−1.012	−1.068	−1.063
SOC-quintets	−1.067	−1.020	−1.105
SSC	−0.371	−0.360	−0.364
total D	−2.45	−2.448	−2.532
exptl	∼−2.3	∼−2.3	∼−2.3

at the experimental geometry can be seen in Table 4. Compared to the results of optical spectroscopy on Tutton's salts,[13] overall good agreement is obtained. First of all, there is the band due to splitting of the ^5E_g state around 8000 cm^{-1} that is correctly reproduced by the calculations. Second, there are two sharp bands assigned to spin-flip transitions observed at ∼17 000 and ∼20 000 cm^{-1}. These are calculated close to 15 000 and 20 000 cm^{-1}, respectively, and are indeed seen to be due to spin-flip transitions. Finally, there is an additional band centered around 14 550 cm^{-1} with a shoulder observed at ∼18 050 cm^{-1}. This band has been assigned[13] as a transition from the ground state to the components of the $^5T_{2g}$ term. Our calculations predict these three peaks in the region from 13 129 to 13 628 cm^{-1}, which agrees well with the observed main feature centered at 14 500 cm^{-1}. However, the calculations do not support the assignment of the 18 050 shoulder to the split $^5T_{2g}$ term. Such a large splitting due to anisotropic π interactions arising from weakly π-bonding water ligands appears to be rather large, and the error of the SORCI method for d−d transitions is typically significantly smaller than ∼4000 cm^{-1}.[45] Alternatively, coupling of internal vibrations of the water molecules with the "d−d" transitions have been held responsible for the observed spectra feature at 18 050 cm^{-1}.[4]

In the initial state average CASSCF calculation, all triplet and quintet states arising from the d^4 configuration were included, but for clarity only the first eight triplet

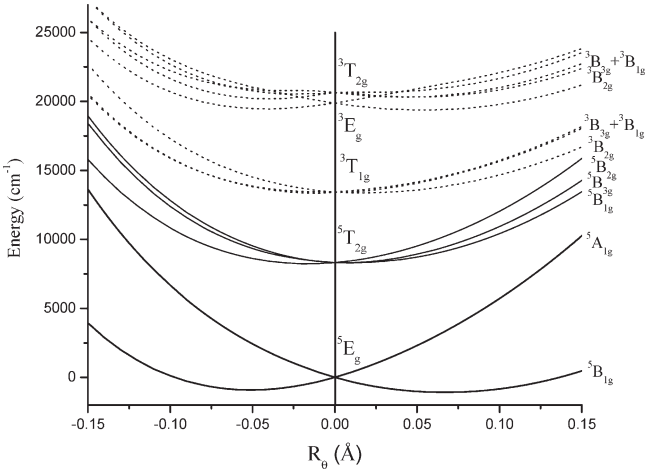

Figure 5. Energy spectrum for the lower electronic states of $Cr(H_2O)_6^{2+}$, along the path of the e_θ normal mode of vibration. The calculations were performed using CASSCF(4,5) and the TZVPP basis set.

states are shown here. These are also the most important ones for determining the value of D. In Table 3, the contributions to the total D value from the different states are analyzed in O_h language; for example, contributions arising from a common T term are summed up for the CASSCF case as well as for the two multireference methods SORCI[29] and MR-DDCI2[28] with the TZVPP basis set. In Table 5, all contributions to the SOC part of D are analyzed for the CASSCF case. It follows from Table 5 that the $^5T_{2g}$ and the first $^3T_{1g}$ states make the most important contributions to the D value, consistent with common belief.[2] However, the second $^3T_{2g}$ state should also not be ignored. The effect of this state was supposed to be non-negligible, but it was speculated that there would probably be a cancelation from the other triplets of the t_2^3e electronic configuration. From our calculations, it turned out that this is not the case, and $^3T_{2g}$ adds another 0.25 cm^{-1} (at the CASSCF level) to the total value of D. From Table 3, it is also obvious that already the CASSCF method can be adequate for the calculation of ZFS. The values calculated for $Cr(H_2O)_6^{2+}$ are in good agreement with those delivered by the much

(45) Neese, F.; Petrenko, T.; Ganyushin, D.; Olbrich, G. *Coord. Chem. Rev.* **2007**, *251*, 288.

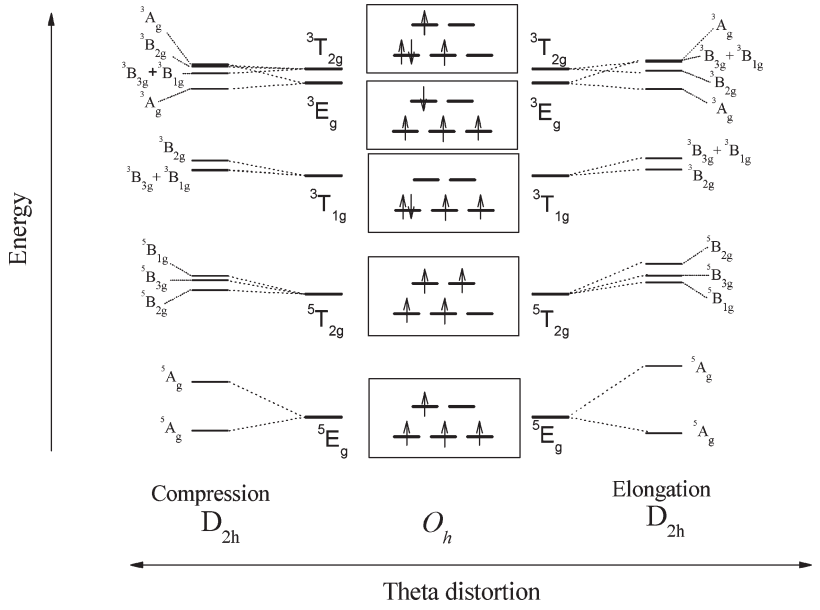

Figure 6. Dependence of the term energies on the D_{4h} distortion coordinate e_θ.

Table 4. Excited States of $Cr(H_2O)_6^{2+}$ Calculated at the SORCI/TZVPP Level of Theory on the Experimental Geometry and the Experimentally Observed Ones

state	SORCI, TZVPP	experiment[13]
^5E_g	0.0	~8000
	7869	
$^5T_{2g}$	13129	14050 + 18050 shoulder
	13507	
	13628	
$^3T_{1g}$	15056	~17000
	15094	
	15106	
$^3T_{2g} + {}^3E_g$	20085	~20000
	20466	
	20495	
	21603	
	22079	

Table 5. Decomposition of Spin−Orbit Part D $Cr(H_2O)_6^{2+}$ as a Sum of Contributions from Different Excited States with the CAS-SCF(4,5) Method and TZVPP Basis Set

		elongation	compression
state in O_h	state in D2h	contribution to D (cm^{-1})	contribution to D (cm^{-1})
$^3T_{2g}$	$^3B_{3g}$	−0.12	−0.07
	$^3B_{2g}$	−0.12	−0.09
	$^3B_{1g}$	0.01	0.08
	sum	−0.25	−0.08
$^3T_{1g}$	$^3B_{3g}$	−0.37	1.04
	$^3B_{2g}$	−0.40	−0.10
	$^3B_{1g}$	0.0	0.0
	sum	−0.77	0.94
$^5T_{2g}$	$^5B_{3g}$	0.17	0.58
	$^5B_{2g}$	0.15	0.65
	$^5B_{1g}$	−1.4	0.0
	sum	−1.24	1.23

more elaborate multireference dynamic correlation methods.

Comparison to Density Functional Theory. In addition to the ab initio calculations, some DFT calculations were also performed at the minimum energy structures with the idea to evaluate the performance of DFT for systems like the present one. Two representative functionals, the hybrid B3LYP[21] functional and the nonhybrid BP86[22−24] functional, together with two different approaches for the estimation of the SOC part have been performed. Both the Pederson and Khanna formula (SOC-PK[46]) and the more recently developed linear response approach[47] were used.

Table 6. Decomposition of the Total Value of D to Its Components Calculated with B3-LYP and BP-86 Functionals with the TZVP Basis Set and Both SOC Operators PK and CP-SOC

		$Cr(H_2O)_6^{2+}$			$Cr(H_2O)_6^{3+}$		
functional	method	SOC	SSC	total	SOC	SSC	total
B3LYP	CP	−0.615	−1.083	−1.670	0.000	0.000	0.000
	PK	−0.554	−1.083	−1.638	0.000	0.000	0.000
BP86	CP	−0.948	−1.045	−1.994	0.000	0.000	0.000
	PK	−0.831	−1.045	−1.876	0.000	0.000	0.000
CASSCF		−2.2	−0.38	−2.58	0.000	0.000	0.000

The results of the calculations can be seen in Table 6. It is obvious that all four combinations of methods and functionals underestimate the total value of D. The CP-SOC[47] method gives better results than the PK approach, for both functionals. In combination with the nonhybrid BP functional, the best result is only ~0.3 cm^{-1} off the experimental value. These results nicely agree with our previous findings, showing that the better theoretical foundation of the CP-SOC method compared to the PK[48] treatment also translates into better numerical performance. However, compared to the ab initio results, it appears that the DFT calculations overestimate the importance of the SSC contribution and underestimate the SOC terms. This type of error cancellation has frequently been observed in DFT calculations of zero-field splitting.

(46) Pederson, M. R.; Khanna, S. N. *Phys. Rev. B* **1999**, *60*, 9566.
(47) Neese, F. *J. Chem. Phys.* **2007**, *127*, 1641.
(48) Zein, S.; Duboc, C.; W., L.; Neese, F. *Inorg. Chem.* **2008**, *47*, 134.

Conclusions

In this work, the zero-field splitting of the di- and trivalent chromium−hexaquo complexes was analyzed with the help of multiconfigurational ab initio quantum chemistry. The divalent $[Cr(H_2O)_6]^{2+}$ system is Jahn−Teller active, and it is therefore necessary to treat the Jahn−Teller effect at some level of sophistication in order to obtain realistic results for the zero-field splitting parameters. State-averaged CASSCF calculations along the Jahn−Teller distortion coordinates provide Jahn−Teller parameters, such as quadratic vibronic couplings, in reasonable agreement with the experimental estimates, even though the intra-^{5}E splitting is underestimated. Results for the optical spectrum that closely match experimental results are obtained by taking care of the dynamic electron correlation using the SORCI or MR-DDCI2 methods and by performing the calculations at the experimental geometry. Calculation of the D value at one of the three equivalent minima using quasi-degenerate perturbation theory in conjunction with correlated multireference methods (SORCI, MR-DDCI2) yielded results in excellent agreement with the experimental findings. Further improvements are obtained if the experimental geometry is used. This then enables the determination of the individual contributions to the D value. The detailed analysis shows that the direct spin−spin coupling makes a contribution of 15% to the total D value, which is not completely negligible but not as large as previously observed for $[Mn(acac)_3]$.[6] Among the ligand field excited states, the quintet state does of course make a significant contribution to the SOC part of the D value, but not as dominant as might have been expected—it is just 44% at the SA-CASSCF level. The second-largest contribution arises from the spin-triplet, spin-flip components. Here, we find that not only the lowest $^3T_{1g}$ state contributes, as assumed in many ligand field treatments, but also the higher-lying triplets make sizable contributions (∼11% of the total value). The use of multireference ab initio methods seems to improve the description of these contributions. Furthermore, it has been shown that second-order perturbation theory is fully adequate for treating the SOC and SSC terms. DFT methods performed somewhat less well than the ab initio approaches, with the best results in the present case being delivered by the nonhybrid BP86 functional in conjunction with linear response theory for the estimation of the SOC contribution to the **D** tensor. In this case, the D value is only underestimated by about 13%.

Unlike the case found for $[Cr(H_2O)_6]^{2+}$, there are no distorting forces for $[Cr(H_2O)_6]^{3+}$, and the structure remains very close to cubic. Consequently, the D value is very small and will be sensitive to small geometrical distortions and environmental effects. Already, a deviation of about 2 pm away from the cubic structure is sufficient to explain the observed value of $|D| \sim 0.1\ cm^{-1}$.

This study once more adds to the credibility of multireference ab initio methods for the calculation of transition metal zero-field splittings. Already, the multiconfigurational entry level, namely, state-averaged CASSCF with a minimal active space, is a fairly useful technique that can also be extended to larger molecules (our most recent implementation can be efficiently employed for calculations up to probably about 2000 basis functions). Higher accuracy can be obtained, of course, by taking care of dynamic correlation effects on top of the minimal CAS. More efficient techniques for carrying out such calculations need to be developed in order to render them as routine applications.

Acknowledgment. Financial support from the German science foundation (Grant NE/6-1); the priority program 1137 ("molecular magnetism"); and SFBs 624 (Bonn), 813 (Bonn) as well as from the German/Israeli Foundation (Grant I-924-171.9/2006) are gratefully acknowledged.